

7. J. Bergoffen *et al.*, *Science* **262**, 2039 (1993).
8. M. Nishi, N. M. Kumar, N. B. Gilula, *Dev. Biol.* **146**, 117 (1991).
9. G. Valdimarsson, P. A. De Sousa, E. C. Beyer, D. L. Paul, G. M. Kidder, *Mol. Reprod. Dev.* **30**, 18 (1991).
10. P. A. De Sousa, G. Valdimarsson, B. J. Nicholson, G. M. Kidder, *Development* **117**, 1355 (1993).
11. E. C. Beyer, D. L. Paul, D. A. Goodenough, *J. Cell Biol.* **105**, 2621 (1987); E. C. Beyer, J. Kistler, D. L. Paul, D. A. Goodenough, *ibid.* **108**, 595 (1989); P. Meda *et al.*, *Endocrinology* **133**, 2371 (1993); B. Risek and N. B. Gilula, *Development* **113**, 165 (1991); B. Risek, S. Guthrie, N. Kumar, N. B. Gilula, *J. Cell Biol.* **110**, 269 (1990); B. Risek, F. G. Klier, N. B. Gilula, *Development* **116**, 639 (1992); C. P. Ruangvoravat and C. W. Lo, *Dev. Dyn.* **194**, 261 (1992); G. Valdimarsson, P. A. De Sousa, G. M. Kidder, *Mol. Reprod. Dev.* **36**, 7 (1993).
12. A. Nagy, J. Rossant, R. Nagy, W. Abramow-Newerly, J. C. Roder, *Proc. Natl. Acad. Sci. U.S.A.* **90**, 8424 (1993).
13. High levels of Cx43 mRNA were detected in RNA from R1 ES cells by Northern (RNA) blot hybridization (A. G. Reaume *et al.*, data not shown).
14. R. M. Mortensen, D. A. Conner, S. Chao, A. A. T. Geisterfer-Lowrance, J. G. Seidman, *Mol. Cell. Biol.* **12**, 2391 (1992).
15. A. G. Reaume *et al.*, data not shown. ES cells were cultured in suspension culture in medium lacking leukemia inhibitory factor for periods of 1 to 2 weeks.
16. ES cells grown on cover slips were processed for immunofluorescence as described (9, 10). The affinity-purified primary antibody was raised against a synthetic peptide corresponding to amino acids 360 to 382 of the COOH-terminal cytoplasmic domain (37) (provided by D. Laird, McGill University). The secondary antibody was fluorescein isothiocyanate-conjugated goat antibody to rabbit immunoglobulin G (IgG) (ICN Biomedicals). The cells were viewed with a Bio-Rad MRC 600 confocal laser scanning microscope.
17. J. R. McLachlan and G. M. Kidder, *Dev. Biol.* **117**, 146 (1986).
18. V. P. Papaioannou and R. Johnson, in *Gene Targeting: A Practical Approach*, A. L. Joyner, Ed. (Oxford Univ. Press, Oxford, 1993), pp. 107-130.
19. A. G. Reaume *et al.*, data not shown.
20. A midline thoracotomy was performed on killed newborn mice and the thoracic cavity was immersed in 3% paraformaldehyde in phosphate-buffered saline (PBS). After fixation the thorax samples were taken through an alcohol dehydration series and dried in a critical point dryer. The hearts were mounted on Cambridge SEM stubs and coated with gold-palladium in a sputter coater. Samples were viewed in a JEOL JSM-840 SEM.
21. Standard techniques were used to prepare transmission electron micrographs of the mutant hearts. Cardiac muscle cell ultrastructure was indistinguishable between mutant and wild-type hearts.
22. B. L. Langille and S. L. Adamson, *Circ. Res.* **48**, 481 (1981). Corrosion casts of the heart and central arteries were prepared with Batson's 317 methyl methacrylate casting compound (Polysciences, Warrington, PA). The descending thoracic aorta was catheterized retrogradely with PE10 polyethylene tubing that had been heat extruded to reduce its external diameter by 70%. The compound was infused immediately after mixing at a rate of 33  $\mu$ l/min with a Harvard model pump.
23. W. J. Larsen, *Human Embryology* (Churchill Livingstone, New York, 1993).
24. B. Bastide *et al.*, *Circ. Res.* **73**, 1138 (1993); G. I. Fishman, E. L. Hertzberg, D. C. Spray, L. A. Leinwand, *ibid.* **68**, 782 (1991); R. G. Gourdie *et al.*, *J. Cell Sci.* **105**, 895 (1993); D. Gros *et al.*, *Circ. Res.* **74**, 839 (1994); H. L. Kanter, J. E. Saffitz, E. C. Beyer, *ibid.* **70**, 438 (1992); M. J. A. van Kempen, C. Fromaget, D. Gros, A. F. M. Moorman, W. H. Lamers, *ibid.* **68**, 1638 (1991).
25. R. G. Gourdie, C. R. Green, N. J. Severs, R. P. Thompson, *Anat. Embryol.* **185**, 363 (1992).
26. R. G. Gourdie, C. R. Green, N. J. Severs, R. H. Anderson, R. P. Thompson, *Circ. Res.* **72**, 278 (1993).
27. J. E. Saffitz, H. L. Kanter, K. G. Green, T. K. Tolley, E. C. Beyer, *ibid.* **74**, 1065 (1994); R. D. Veenstra, H.-Z. Wang, E. M. Westphale, E. C. Beyer, *ibid.* **71**, 1277 (1992).
28. Quantitative analysis by reverse transcription-polymerase chain reaction was performed on multiple samples of heart tissue isolated from mutant, heterozygous, and wild-type embryos recovered at 16.5 days of gestation.
29. R. Minkoff, V. R. Rundus, S. B. Parker, E. C. Beyer, E. L. Herzberg, *Circ. Res.* **73**, 71 (1993).
30. M. Vuillemin and T. Pexieder, *Am. J. Anat.* **184**, 114 (1989).
31. D. E. Bockman, M. E. Redmond, K. Waldo, H. Davis, M. L. Kirby, *ibid.* **180**, 332 (1987).
32. T. Pexieder, *Adv. Anat. Embryol. Cell Biol.* **51**, 6 (1975); J. M. Hurle and J. L. Ojeda, *J. Anat.* **129**, 427 (1979).
33. S. B. Bishop, P. G. Anderson, D. C. Tucker, *Circ. Res.* **66**, 84 (1990); E. B. Clark *et al.*, *Am. J. Physiol.* **257**, H55 (1989).
34. M. H. El-Fouly, J. E. Trosko, C.-C. Chang, *Exp. Cell Res.* **168**, 422 (1987). Primary embryo fibroblasts were grown to confluence in 35-mm tissue culture dishes, washed with PBS, and then scored with a sharp scalpel blade. The cultures were then incubated in a mixture of 0.2% Lucifer yellow and 0.05% rhodamine dextran (Molecular Probes) in PBS for 5 min in the dark. After rinsing thoroughly in PBS, culture medium was replaced and the cells were allowed to recover for an additional 5 min. Cells were rinsed again, mounted with PBS under glass cover slips, and examined under rhodamine and fluorescence excitation conditions in a Leitz photomicroscope.
35. Protein immunoblotting was performed as described (38). Blots were treated with an affinity-purified rabbit antibody directed against a synthetic peptide corresponding to amino acids 302 to 319 (10) (supplied by B. Nicholson, State University of New York, Buffalo). Bound rabbit antibodies were detected with  $^{125}$ I-labeled goat antibody to rabbit IgG (ICN Biomedicals).
36. S. H. Britz-Cunningham, M. M. Shah, A.-M. Martinez, W. H. Fletcher, *Mol. Biol. Cell.* **4**, 329 (1993).
37. D. W. Laird and J.-P. Revel, *J. Cell Sci.* **97**, 109 (1990).
38. C. C. G. Naus, D. Zhu, S. D. L. Todd, G. M. Kidder, *Cell. Mol. Neurobiol.* **12**, 163 (1992).
39. W. Wurst and A. Joyner, in *Gene Targeting: A Practical Approach*, A. L. Joyner, Ed. (Oxford Univ. Press, Oxford, 1993), pp. 31-62.
40. We thank S. Lye and M. Bennett for useful discussions, K. Harpal for histological preparations, H. Christensen for TEM assistance, E. C. Beyer for pG2A probe, and B. J. Nicholson, D. L. Paul, and D. W. Laird for supplying complementary DNAs, antibodies, and the unpublished mouse Cx43 sequence. Supported by grants from the Medical Research Council (J.R. and B.L.L.) and the Natural Sciences and Engineering Research Council of Canada (NSERC) (G.M.K.). A.G.R. held a National Cancer Institute of Canada postdoctoral fellowship. P.deS. holds an NSERC postdoctoral fellowship. J.R. is a Terry Fox Cancer Research Scientist of the National Cancer Institute of Canada and an International Scholar of the Howard Hughes Medical Institute. The Cx43 mutant mice are available through the Induced Mutant Resource at the Jackson Laboratory, Bar Harbor, ME, USA.

5 August 1994; accepted 11 January 1995

## Kinectin, an Essential Anchor for Kinesin-Driven Vesicle Motility

Janardan Kumar, Harry Yu, Michael P. Sheetz\*

The membrane anchor for the molecular motor kinesin is a critical site involved in intracellular membrane trafficking. Monoclonal antibodies specific for the cytoplasmic surface of chick brain microsomes were used to define proteins involved in microtubule-dependent transport. One of four antibodies tested inhibited plus-end-directed vesicle motility by approximately 90 percent even as a monovalent Fab fragment and reduced kinesin binding to vesicles. This antibody bound to the cytoplasmic domain of kinectin, an integral membrane protein of the endoplasmic reticulum that binds to kinesin. Thus, kinectin acted as a membrane anchor protein for kinesin-driven vesicle motility.

Kinesin and cytoplasmic dynein are ubiquitous mechanochemical adenosine triphosphatases (ATPases) involved in powering diverse forms of intracellular organelle transport such as anterograde and retrograde movements of vesicles along microtubules and a variety of membrane-trafficking events (1, 2). Kinesin directs plus-end (anterograde) movement, whereas cytoplasmic dynein directs minus-end (retrograde) transport. Antibodies specific for kinesin heavy chain inhibit vesicle movements affecting axoplasmic transport or other cellular motile processes (3). These ATPases or motors interact with integral membrane proteins on vesicle surfaces (4, 5) that pre-

sumably contain the vesicle signals (6) regulating the directionality of vesicle movement on microtubules. Protein-dependent motor binding to motile vesicle populations has been quantitated (5), and a kinesin-binding, integral membrane protein has been isolated from motile microsomes (7). It is unclear to what extent motor binding is related to vesicle motility and which motor-binding membrane protein is directly involved in motility. Here we define the effects of specific monoclonal antibodies (mAbs) on the in vitro movement of membranous organelles along microtubules (1, 4, 8, 9) and the binding of kinesin to organelles, presumably through the tail portion of the kinesin heavy chain (5).

Monoclonal antibodies were raised against native epitopes on the cytoplasmic surface of carbonate-washed microsomal

Department of Cell Biology, P.O. Box 3709, Duke University Medical Center, Durham, NC 27710, USA.

\*To whom correspondence should be addressed.

vesicles. Four mAbs were characterized that bound to the cytoplasmic surface of carbonate-washed brain microsomes (Table 1). When we tested the antibodies for their effects on *in vitro* vesicle movement on randomly oriented microtubules (10), only one mAb, termed VSP4D (vesicle surface protein 4D), caused a significant decrease

(~70%) in total vesicle motile activity. Similarly, vesicle attachment to microtubules was inhibited by ~70% in the presence of VSP4D (Table 2). The amount of VSP4D bound to the vesicles was significantly less than the other VSP antibodies that did not block motility (Table 1), ruling out the possibility that the inhibition was due to a mass effect.

**Table 1.** Association of VSP mAbs with carbonate-extracted microsomal vesicles. Binding of five mAbs to carbonate-washed (CW) vesicles from chick embryo brain was quantified by immunoblotting after separation from unbound antibodies by sedimentation (19). Control antibodies of similar isotypes did not show significant binding under these conditions. KR160.9.1 (7) was an anti-kinectin mAb capable of binding to native as well as denatured kinectin. Other mAbs were raised against surface proteins of vesicles. The number of VSP4D antibodies bound to vesicles corresponds to ~2.5 VSP4D molecules per 100-nm vesicle, whereas one to four kinectin molecules per 100-nm vesicle were reported (5, 7). Bound mAbs were expressed as micrograms per milligram of vesicle proteins (mean  $\pm$  SEM from three or four experiments).

mAb	Molecular mass of antigen (kD)	mAb subclass	Bound mAb
VSP4D	160	IgG2a	3.24 $\pm$ 0.40
VSP2B	98; 96	IgG1	27.88 $\pm$ 2.36
VSP9G	43; 208	IgG2a	13.83 $\pm$ 1.19
VSP2H	29	IgG1	12.81 $\pm$ 1.03
KR160.9	160; 120	IgG2b	2.91 $\pm$ 0.37

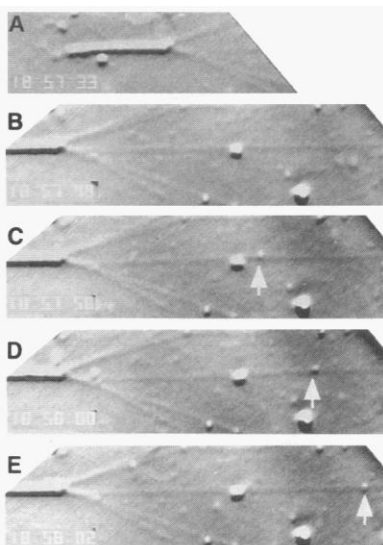


**Fig. 1.** *In vitro* vesicle motility assay on polar microtubules (20). To assess the effects of mAbs on either plus-end (kinesin-driven)– or minus-end (cytoplasmic dynein-driven)–directed vesicle motility in the presence of a high-speed cytoplasmic supernatant of the homogenized chick embryo fibroblast cells, we quantified movements using an axoneme-based motility assay (11). Figure shows a typical plus-end-directed vesicle movement (arrows indicate the positions of the moving vesicle).

To test whether VSP4D inhibited all motility or was specific for kinesin- or cytoplasmic dynein-based motility, we used an *in vitro* vesicle motility assay (11) with microtubules that were polarized by polymerization on axonemes (Fig. 1). The chick embryo fibroblasts were first treated with dibutyl cyclic AMP (1 mM for 1 hour in culture media) before harvesting, which caused a significant increase in overall motility as well as an increase in the plus-end-directed motility (12). The proportion of kinesin-driven vesicles among all motile vesicles was consistent with previous studies (8). The number and direction of vesicle movements were quantified for vesicles preincubated with VSP4D, the control mAb VSP2B, or buffer alone (Table 2). To control for possible antibody cross-linking of vesicles that might reduce the effective concentration of vesicles, we normalized motile activity (the number of observed movements per minute per 36  $\mu$ m of microtubule length) to the free vesicle concentration (the number of diffusing vesicles observed per 4  $\mu$ m<sup>2</sup> of buffer per minute). Plus-end-directed motility (kinesin-driven) was inhibited by ~90% by VSP4D even when the monovalent Fab fragment was used (Table 2). Minus-end-directed motility was also inhibited but not to the same extent (particularly as the Fab), indicating that the effect of VSP4D was preferential for plus-end- or kinesin-driven motility. None of the antibodies had any effect on the velocity of the vesicle movements toward plus-end (~2  $\mu$ m/s) or minus-end (~3  $\mu$ m/s). The control antibody, VSP2B,

had no significant effect on motility in either direction (Table 2) even though more VSP2B antibody bound to the vesicle surface than VSP4D (Table 1). Thus, the binding of VSP4D to the cytoplasmic surface of vesicles specifically inhibited microtubule-dependent vesicle motility driven by kinesin.

Because VSP4D was raised against a vesicle membrane protein, it is conceivable that inhibition of the vesicle motility is caused by a disruption of the attachment of motors to their membrane anchors. To test this hypothesis, we used a motor-vesicle binding assay (5) to measure the effect of VSP4D on the binding of kinesin to carbonate-washed chick embryo brain dense microsomes (Fig. 2). VSP4D inhibited kinesin binding by 70  $\pm$  2.9%, whereas VSP2B on the same vesicles did not affect kinesin binding to the vesicles. The inhibition of kinesin binding to vesicles by VSP4D seems less than the level of its inhibition of the plus-end-directed vesicle motility. This difference could be explained by a small population of additional kinesin binding sites on microsomes that were not directly involved in organelle motility. We conclude that the antigen for VSP4D was the major membrane anchor for kinesin binding to vesicles.

The antigen for VSP4D was examined in an electroblot of the microsomal proteins, but no vesicle membrane proteins reacted with VSP4D. However, renaturation of vesicle proteins on nitrocellulose with lecithin vesicles did enable VSP4D to react weakly with a band of 160 kD (13). We then immunoprecipitated the antigen after labeling the cytoplasmic portions of the carbonate-washed vesicle membrane proteins with an impermeant reagent, sulfo-succinimidobiotin. When antibody-coated vesicles were detergent solubilized and the antibody precipitated by protein A beads, a single biotinylated protein of 160 kD was detected (Fig. 3), which was identified as

**Table 2.** Monoclonal antibody inhibition of microtubule-based vesicle motility. Anti-kinectin mAb VSP4D was incubated with chick embryo fibroblast vesicles (0.1 mg of mAb per 0.2 mg of vesicle proteins), and the vesicles were used in a directionality motility assay (Fig. 1). The vesicle movements were compared with controls (no mAb and VSP2B). The number of movements per minute is the normalized number of moving vesicles per 36- $\mu$ m microtubule length per (70 vesicles in 4  $\mu$ m<sup>2</sup> of buffer per minute). *n* is the number of fields analyzed, and each field was measured from 1 to 3 min so that the time measured ranged from 32 to 92 min. The normalized number of vesicles attached is the sum of the number of stationary and moving vesicles attached to 36  $\mu$ m of microtubule length.

mAb	Vesicle movements (no. of movements per minute $\pm$ SEM)		No. of vesicles attached ( <i>n</i> )
	Plus-end directed	Minus-end directed	
Control	2.32 $\pm$ 0.35	13.98 $\pm$ 1.12	25.12 $\pm$ 2.30 (60)
VSP2B whole IgG	2.87 $\pm$ 0.75	11.48 $\pm$ 0.95	23.54 $\pm$ 2.89 (24)
VSP2B Fab	2.30 $\pm$ 0.87	10.04 $\pm$ 1.20	17.59 $\pm$ 3.21 (24)
VSP4D whole IgG	0.23 $\pm$ 0.08	4.37 $\pm$ 0.36	7.72 $\pm$ 0.97 (35)
VSP4D Fab	0.15 $\pm$ 0.06	6.61 $\pm$ 1.10	10.8 $\pm$ 2.75 (33)

kinectin by anti-kinectin mAb KR 160.9.1 (7) (Fig. 3). In addition, a bacterially expressed clone of kinectin reacted with VSP4D, whereas control proteins did not (14). Several proteins precipitated by VSP4D were unbiotinylated (probably luminal), including one of ~300 kD and two to three diffuse bands of ~60 to 70 kD (Fig. 3, lane 2). The control antibody, VSP2B, immunoprecipitated a doublet of biotinylated proteins of 98 and 96 kD but not the luminal proteins (Fig. 3, lane 7). Thus, VSP4D immunoprecipitated only kinectin from the cytoplasmic surface of vesicles, and several luminal proteins appeared to be selectively associated.

Here we have shown that an antibody to kinectin specifically inhibits kinesin-depen-

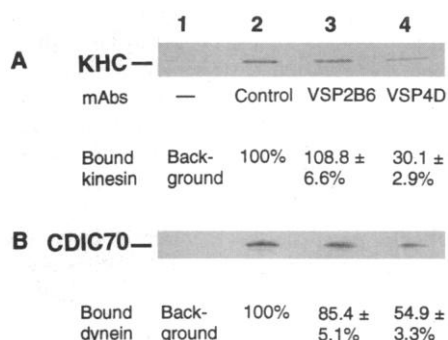


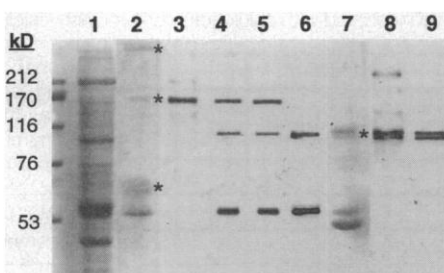
**Fig. 2.** Effect of mAbs on motor binding to CW vesicles (19). (A) A sample blot from a typical kinesin-binding experiment with a table (below) summarizing the results from three sets of data. (B) A sample blot from a typical cytoplasmic dynein binding experiment with a table (below) summarizing the results from three sets of data. Lane 1, background level of the motor association with vesicles; lane 2, control (no antibody added); lane 3, motor binding to VSP2B-coated vesicles; and lane 4, motor binding to VSP4D-coated vesicles. KHC is the kinesin heavy chain that binds to vesicles and is quantified with mAb 9E5.KHC2 (5) on immunoblot. CDIC70 is the 70-kD intermediate chain of cytoplasmic dynein that binds to vesicles and is quantified with mAb 70.1 (22). Percentages were calculated relative to the control (mean ± SEM).

**Fig. 3.** Immunoprecipitation of antigens from biotinylated CW vesicles by mAbs (21). The immunoprecipitates were analyzed by SDS-PAGE and visualized by Coomassie blue (CB) (lanes 1, 2, and 7) and immunoblotting (lanes 3 to 6, 8, and 9). Lane 1, Coomassie blue-stained protein profile of vesicles; lane 2, CB-stained VSP4D immunoprecipitate; lane 3, blot of the VSP4D immunoprecipitate stained with Avidin-alkaline phosphatase (Avidin-AP); lane 4, blot of the VSP4D immunoprecipitate stained with anti-kinectin mAb KR160.9.1 (7); lane 5, blot of the VSP4D immunoprecipitate stained with KR160.9.1 and Avidin-AP; lane 6, blot of the VSP4D immunoprecipitate stained with secondary antibody alone, which yields a 100-kD band. When KR160.9.1 was used to react with CW vesicles on immunoblot, it reacted with only the 160-kD kinectin (7), indicating that the 100-kD band is not a CW vesicle protein. It is likely to be a partially unreduced IgG molecule in the immunoprecipitation complex. Lane 7, CB-stained VSP2B immunoprecipitate; lane 8, blot of the VSP2B immunoprecipitate stained with Avidin-AP; and lane 9, vesicle proteins stained with VSP2B. \*, indicates bands of interest as described in text.

dent vesicle motility even as a Fab fragment, suggesting that kinectin is an essential membrane anchor for kinesin-driven motility. The other antibodies, which bound to the vesicles in equal or greater amounts than VSP4D, had no effect on motility. Because VSP4D also inhibited the majority of kinesin binding to motile microsome, we suggest that the mechanism of inhibition of motility is through blocking of the kinesin binding site on kinectin. Further support of this hypothesis is provided by the observation of a direct interaction between kinesin and bacterially expressed kinectin (14).

Cytoplasmic dynein-dependent vesicle motility was also inhibited by ~50% by VSP4D (Table 2). This inhibition of minus-end-directed vesicle motility by VSP4D was accounted for by a similar level of inhibition of cytoplasmic dynein binding to vesicles (Fig. 2). We suggest that VSP4D inhibited minus-end-directed vesicle motility by blocking the cytoplasmic dynein binding site on or adjacent to kinectin. The extent of inhibition was less (especially with the Fab fragment) than kinesin-dependent motility, implying that the VSP4D epitope is displaced from the cytoplasmic dynein binding site on kinectin or that a separate protein binds cytoplasmic dynein in the neighborhood of kinectin. Earlier studies suggested that kinesin and cytoplasmic dynein bound to neighboring sites on these vesicles (5). Further studies are under way to determine if bacterially expressed kinectin, which binds kinesin, will also bind cytoplasmic dynein. If both motors bind to adjacent sites on kinectin, then a single modification of kinectin might switch directionality of movement.

Alternative models have been proposed to explain the interactions of motor proteins with the cytoplasmic surface of vesicles in other systems. Motor binding to vesicle lipids or membrane-associated tubulin (5, 15) has been suggested on the basis of the interaction of cytoplasmic dynein



with lipids and kinesin with tubulin. In the case of another motor, myosin I, the tail domain is responsible for interaction with acidic phospholipids (16), but it is unclear whether myosin I binds to a protein receptor in addition to this lipid binding. In the chick vesicles we have not detected any kinesin binding to membrane-associated tubulin or lipids (5). Kinectin can account for the majority of the kinesin binding sites found on motile microsome (7), and the recent cloning and sequencing of kinectin has confirmed that it is an integral membrane protein of the endoplasmic reticulum (14). We suggest that kinectin is the kinesin receptor for organelle motility and may be involved in the control of direction of movement on microtubules.

## REFERENCES AND NOTES

1. M. Bomsel, R. Parton, S. A. Kuznetsov, T. A. Schroer, J. Gruenberg, *Cell* **62**, 719 (1990); T. A. Schroer and M. P. Sheetz, *Annu. Rev. Physiol.* **53**, 629 (1991); S. T. Brady, *Neuron* **7**, 521 (1991).
2. R. B. Vallee and H. S. Shpetner, *Annu. Rev. Biochem.* **59**, 909 (1990); R. A. Walker and M. P. Sheetz, *ibid.* **62**, 429 (1993).
3. P. J. Hollenbeck and J. A. Swanson, *Nature* **346**, 864 (1990); S. T. Brady, K. K. Pfister, G. S. Bloom, *Proc. Natl. Acad. Sci. U.S.A.* **87**, 1061 (1990); V. I. Rodionov, F. K. Gyoeva, V. I. Gelfand, *ibid.* **88**, 4956 (1991); V. I. Rodionov et al., *J. Cell Biol.* **123**, 1811 (1993); R. A. Steinhart, G. Bi, J. M. Alderton, *Science* **263**, 390 (1994).
4. J. K. Burkhardt, J. M. McIlvain Jr., M. P. Sheetz, Y. Argon, *J. Cell Sci.* **104**, 151 (1993).
5. H. Yu, I. Toyoshima, E. R. Steuer, M. P. Sheetz, *J. Biol. Chem.* **267**, 20457 (1992); D. A. Skoufias, D. G. Cole, K. P. Wedaman, J. M. Scholey, *ibid.* **269**, 1477 (1994).
6. M. P. Sheetz, R. D. Vale, B. J. Schnapp, T. A. Schroer, T. S. Reese, *J. Cell Sci. Suppl.* **5**, 181 (1986).
7. I. Toyoshima, H. Yu, E. R. Steuer, M. P. Sheetz, *J. Cell Biol.* **118**, 1121 (1992).
8. T. A. Schroer, E. R. Steuer, M. P. Sheetz, *Cell* **56**, 937 (1989); J. M. McIlvain Jr., J. K. Burkhardt, S. Hamm-Alvarez, Y. Argon, M. P. Sheetz, *J. Biol. Chem.* **269**, 19176 (1994).
9. B. J. Schnapp and T. S. Reese, *Proc. Natl. Acad. Sci. U.S.A.* **86**, 1548 (1989).
10. T. A. Schroer, B. J. Schnapp, T. S. Reese, M. P. Sheetz, *J. Cell Biol.* **107**, 1785 (1988).
11. T. A. Schroer and M. P. Sheetz, *ibid.* **115**, 1309 (1991); A. Hyman et al., *Methods Enzymol.* **196**, 478 (1991).
12. S. Hamm-Alvarez, P. Kim, M. P. Sheetz, *J. Cell Sci.* **106**, 955 (1993).
13. J. Kumar, H. Yu, M. P. Sheetz, unpublished data.
14. H. Yu et al., *Mol. Biol. Cell*, in press.
15. M. L. Lacey and L. T. Haimo, *Cell Motil. Cytoskeleton* **28**, 205 (1994).
16. R. J. Adams and T. D. Pollard, *Nature* **340**, 565 (1989).
17. E. Harlow and D. Lane, *Antibodies, A Laboratory Manual* (Cold Spring Harbor Laboratory, Cold Spring Harbor, NY, 1988).
18. U. K. Laemmli, *Nature* **227**, 680 (1970).
19. Carbonate-washed [CW; 0.1 M Na<sub>2</sub>CO<sub>3</sub> (pH 11.3)] chick embryo brain vesicles were prepared (7) and used to immunize each of five mice with three boosts of 100 to 150 µg of vesicle protein per mouse (5). The mAbs to native epitopes were selected by enzyme-linked immunosorbent assay screening against CW vesicles and were subcloned to give monoclonal lines. In immunoblots of vesicle proteins, three of the mAbs reacted with single or closely spaced doublet bands (VSP2B with bands of 96 and 98 kD, VSP9G with predominant bands of 43 and 208 kD, and VSP2H

with a band of 29 kD). A fourth mAb was found that did not react with standard immunoblots but did bind to intact vesicles (VSP4D). Ascites production, immunoglobulin G (IgG) purification, and Fab fragment isolation were performed according to standard procedures (17). For quantitation of antibody binding to CW vesicles, the vesicles were mixed with 3% bovine serum albumin (BSA) (fatty acid-free; Sigma) for 1 hour at 4°C. Vesicles (10 to 20 µg of vesicle proteins) in a total volume of 200 µl were mixed overnight at 4°C with 0.2 to 0.3 mg of antibodies (ascites) per milliliter or a control mouse IgG. Each sample was layered onto a three-step sucrose gradient (100 µl of 15%, 200 µl of 10%, and 200 µl of 5% sucrose in homogenization buffer) and centrifuged at 4°C for 20 min with an SW-55Ti rotor at 192,000g. The supernatant and the sucrose were removed completely and the pellet was resuspended in 25 µl of electrophoresis sample buffer (18) with an additional 1% SDS and analyzed as described (5). The effect of antibody on motor binding to vesicles was measured with VSP4D and VSP2B (control) as described (5, 7) with slight modification. CW vesicles (2.0 to 3.0 µg of vesicle proteins for kinesin binding and 5 µg for dynein binding) in a total volume of 60 µl of PMEE' buffer [35 mM K-Pipes (pH 7.4), 5 mM MgCl<sub>2</sub>, 5 mM EGTA, and 0.5 mM EDTA] were mixed with IgG (0.16 to 0.25 mg/ml for kinesin binding and 0.42 mg/ml for dynein binding) on ice for 1 hour and 10 to 15 min at 37°C before addition of a purified motor fraction [10 to 20 nmol of motors prepared as described in (8)]. The binding experiments were performed as described (5). Binding of motors was inhibited by VSP4D, whereas no effect was observed with VSP2B.

20. The *in vitro* vesicle motility assay on polar microtubules was performed after preparation of cytosolic fractions and CW chick embryo fibroblast vesicles as described (8, 11). Sea urchin sperm axonemes were a gift from T. Salmon (University of North Carolina at Chapel Hill, NC). Porcine tubulin (1×) and *N*-ethylmaleimide-treated tubulin (2×) were mixed and diluted to ~3.0 mg/ml final concentration with PMEE' and 1 mM guanosine triphosphate (GTP). Axonemes were added to an acid-washed cover slip in a flow cell formed with two parallel strips of double-sided tape and a glass slide for 2 min at a concentration of ~2 per video field (~500 µm<sup>2</sup>). The tubulin mixture was exchanged into the flow cell and incubated in a humidity chamber at 37°C for 15 min. The free tubulin was washed out with PMEE', 1 mM GTP, and 20 µM Taxol. CW vesicles (0.2 mg/ml) were reacted with mAbs (0.1 mg/ml) for 2 to 3 hours with rocking at 4°C. To measure motility, we incubated the mixture of vesicles and antibodies with a cytosolic fraction (S3) and 5 mM Mg-ATP, and then added the mixture to the polarized microtubules in a flow cell. Samples were observed on a heated Zeiss Axiovert-100 microscope at 35° to 37°C by video-enhanced differential interference contrast, and motility was analyzed as described (5). The number of vesicle movements was normalized to the concentration of vesicles in the medium and the length of microtubules in the field [expressed as movements per minute per 36 µm of microtubule length (per 70 vesicles in 4 µm<sup>2</sup> of buffer per minute)]. Moving vesicles are counted only once after they bind and move (stopping and restarting is not counted as a second movement). Vesicles do not reverse direction of movements. Means and standard error of means (SEM) were calculated and weighted by the number of minutes analyzed for each field.
21. To identify the antigen for VSP4D, we biotinylated CW vesicles as described (7). Biotinylated vesicles were collected at a 15/60% sucrose interface after centrifugation at 192,000g for 30 min (Beckman SW55Ti rotor) and were dialyzed against PMEE' before incubation with 3% BSA at 4°C for 1 hour. The vesicles were then mixed with the designated antibody for 5 hours at 4°C and collected at a 15/60% sucrose interface after centrifugation. The vesicles were solubilized with 1% Triton X-100 and 0.5 M NaCl and centrifuged at 150,000g for 30 min in a TLA100.2 rotor. The supernatants were incubated with protein A-Sepharose CL-4B (Schleicher & Schuell) for 4 to 5 hours at 4°C and washed four times with NET buffer [150 mM NaCl,

50 mM tris-HCl, 5 mM EDTA (pH 8.0)]. The immunoprecipitates were solubilized directly in electrophoresis sample buffer (18) and analyzed by SDS-polyacrylamide gel electrophoresis (PAGE) and immunoblotting.

22. E. R. Steuer, L. Wordeman, T. A. Schroer, M. P. Sheetz, *Nature* **345**, 266 (1990).
23. We thank J. Lockman for assisting in mAb produc-

tion, J. Mellvain for help with microscopy, and Z. Wang for help with the motility assay. We also thank J. Lippincott-Schwartz and H. P. Erickson for comments on the manuscript, and members of the Sheetz lab for discussions. Supported by grant NS 23345 from the National Institutes of Health.

19 September 1994; accepted 9 December 1994

## 1/f Noise in Human Cognition

D. L. Gilden,\* T. Thornton, M. W. Mallon

When a person attempts to produce from memory a given spatial or temporal interval, there is inevitably some error associated with the estimate. The time course of this error was measured in a series of experiments where subjects repeatedly attempted to replicate given target intervals. Sequences of the errors in both spatial and temporal replications were found to fluctuate as *1/f* noises. *1/f* noise is encountered in a wide variety of physical systems and is theorized to be a characteristic signature of complexity.

Of the types of activity that characterize physical systems, perhaps the most ubiquitous and puzzling is the appearance of *1/f* noise, a form of temporal fluctuation that has a power density inversely proportional to the frequency (that is, power ~ *1/f*). *1/f* noise, also known as pink or flicker noise, varies with a predictability intermediate between white noise (no correlation in time, power ~ *1/f*<sup>0</sup>) and Brownian motion (no correlation between increments, power ~ *1/f*<sup>2</sup>). *1/f* noise has been observed in a profusion of domains as diverse as condensed matter systems (1, 2), traffic flow (3), quasar emissions (4), river discharge (5), DNA base sequence structure (6), and cellular automata (7). This list is hardly exhaustive, as entire symposia are devoted to its occurrence and causation (8). The universality of *1/f* noise suggests that it does not arise as the consequence of particular physical interactions, but instead is a general manifestation of complex systems. Here we present evidence that *1/f* noises are associated with certain basic aspects of human cognition: the representation of spatial and temporal intervals.

Despite the interest in complex systems within the social sciences, there have been few examples of *1/f* noise reported in human or animal behavior (9). Most notably, music and speech have been shown to have *1/f* fluctuations in both pitch and loudness (10). The occurrence of *1/f* noise in these contexts, however, should be distinguished from its appearance in purely physical systems. Pitch and loudness carry information in music and speech signals and are therefore subject to the constraints that exist generally in communication. Their spectral

properties may be due to the fact that *1/f* noise represents an optimal compromise between efficient transfer of information (maximized by white noise) and immunity to error (6).

Our investigations concern the production of spatial and temporal intervals. The experiments we conducted were extremely simple. Subjects were first given an example of a target spatial or temporal interval and then made, to the best of their ability, a series of replicates. The errors in replication were treated as a time series and were submitted to Fourier analysis. Figure 1 illustrates the power spectra of the errors deriving from the estimation of temporal intervals. Results from six experiments are displayed in which the target time interval varied between 0.30 and 10 s in duration (Fig. 1A). These power spectra share a family resemblance that is distinguished by the presence of two features. All the spectra are *1/f* at frequencies less than about 0.2 Hz, and there is a quadratic trend at higher frequencies that becomes progressively more pronounced with shorter target durations.

The overall coherence of this data set suggests that it may be understood in terms of a few simple mechanisms. Earlier work on timing variance (11) presented evidence for a model in which the production of temporal intervals is composed of two parts: an internal clock (C) that mediates the judgment of time passage, and a motor program that actuates the responses which signal the beginning and ending of each interval. The motor program in this model does not operate instantaneously, and all responses have an assigned motor delay (MD). In terms of these two components, the *j*th observed interval *I<sub>j</sub>* is written as

$$I_j = C_j + MD_j - MD_{j-1}$$

The difference in motor delays arises from

Department of Psychology, University of Texas at Austin, Austin, TX 78712, USA.

\*To whom correspondence should be addressed.